ISSN 1070-3284, Russian Journal of Coordination Chemistry, 2020, Vol. 46, No. 2, pp. 89–97. © Pleiades Publishing, Ltd., 2020.
Russian Text © The Author(s), 2020, published in Koordinatsionnaya Khimiya, 2020, Vol. 46, No. 2, pp. 81–90.

Coordination Polymers Based on Oxovanadium(IV) Butylmalonate Fragments and Potassium, Magnesium, and Cadmium Cations

E. S. Bazhina[a, *], G. G. Aleksandrov[a, †], M. A. Kiskin[a], A. A. Sidorov[a], and I. L. Eremenko[a]
[a] *Kurnakov Institute of General and Inorganic Chemistry, Russian Academy of Sciences, Moscow, 119991 Russia*
**e-mail: evgenia-VO@mail.ru*

Received September 4, 2019; revised September 18, 2019; accepted September 23, 2019

Abstract—The data on the synthesis and study of the crystal structure of compounds $\{[K_2Mg_2(VO)_3(Bumal)_6(H_2O)_{15}] \cdot 2H_2O\}_n$ (**I**) and $\{[Cd(VO)(Bumal)_2(H_2O)_5] \cdot H_2O\}_n$ (**II**) are presented. According to X-ray diffraction, these compounds are formed by the anionic fragments $[VO(Bumal)_2(H_2O)]^{2-}$ with oxovanadium(IV) and two butylmalonate anions (H_2Bumal is $C_5H_{10}(COOH)_2$) coordinated via the chelate mode. In the crystals of compound **I** (CIF file CCDC no. 1911220), the $[VO(Bumal)_2(H_2O)]^{2-}$ anionic fragments are bound to each other by the K^+ and Mg^{2+} cations into the 2D polymeic structure. In compound **II** (CIF file CCDC no. 1033008), these fragments are bound by the Cd^{2+} cations to form the 1D coordination polymer.

Keywords: oxovanadium(IV), butylmalonic acid, heterometallic complexes, coordination polymers, X-ray structure analysis

DOI: 10.1134/S1070328420020025

INTRODUCTION

Anions of carboxylic acids are capable of manifesting diverse coordination modes and, hence, they are convenient for the design of polynuclear transition metal complexes with the magnetic [1–7] and/or luminescence properties [8–14]. They also exhibit catalytic [15, 16] and biological activities [17]. Bridging anions of dicarboxylic acids find wide use in the construction of porous metal-organic frameworks capable of selective sorption of small molecules and ions [18–26]. Substituted malonic acids (H_2R_2mal) play a special role among the representatives of this large class of ligands, since their anions are capable of forming six-membered chelate cycles with 3*d*-metal cations and, correspondingly, can form stable mononuclear bis-chelate anionic complexes $[M(R_2mal)_2]^{2-}$ ($M = VO^{2+}$, Co^{2+}, Ni^{2+}, Cu^{2+}, Zn^{2+}) containing free for coordination oxygen atoms of carboxyl groups. These complexes are promising as metal-containing blocks for assembling polynuclear structures and coordination polymers containing metal atoms of various types [27, 28]. The nature of substituents (R) in a malonate anion affects not only the solubility of the reaction product in a specific reaction medium but its crystal structure. In addition, cations of alkaline (M') and alkaline-earth (M") metals introduced into the reaction as a salt of substituted malonic acid play the structure forming role in the malonate systems. In the most part of cases, the radius of these cations in combination with the size of the substituent of the malonate ligand determines the dimensionality of the formed polymeric structures $[M''_2M(R_2mal)_2]_n$ and $[M''M(R_2mal)_2]_n$ (M is a 3*d*-metal cation) [29]. A doubtless advantage of these compounds is the possibility of substituting alkaline and alkaline-earth metal cations by double-charged cations of magnesium and various *d* metals, resulting in the formation of new heterometallic compounds with different compositions and structures. For example, the reactions of compounds $\{[Ba(VO)\text{-}(Me_2mal)_2(H_2O)] \cdot H_2O\}_n$ and $\{[Ba_3(VO)_3(Bumal)_6\text{-}(H_2O)_{13}] \cdot 4H_2O\}_n$ with manganese(II) sulfate in aqueous solutions led to the complete substitution of the barium(II) cations by manganese(II) cations to form 1D polymers $\{[Mn(VO)(R_2mal)_2(H_2O)_5] \cdot H_2O\}_n$ (R_2 is Me_2 or Bu, respectively) [30]. In the case of the heterometallic K–M complexes, both the complete and partial substitution of potassium ions is possible. The partial substitution of potassium cations by the corresponding metal cations was demonstrated for the reactions of $[K_4(VO)_2(Cbdc)_4(H_2O)_4]_n$ with magnesium nitrate and $[K_8Cu_4(Me_2mal)_8(H_2O)_8]_n$ with magnesium, nickel(II), or cobalt(II) nitrates [31, 32], whereas the reaction of $[K_8Cu_4(Me_2mal)_8(H_2O)_8]_n$ with cadmium

---

[†] Deceased.

nitrate afforded the product of complete substitution of the potassium cations by cadmium [33].

The possibilities of the substitution of K^+ cations by cations of Mg^{2+} and *d* metals (Mn^{2+}, Cd^{2+}) in the reaction of vanadyl sulfate and butylmalonic acid potassium salt in a ratio of 1 : 2 were studied in this work. Two new oxovanadium(IV) compounds were isolated as single crystals and studied by X-ray diffraction analysis: the product of the partial substitution of potassium cations by magnesium, 2D polymer $\{[K_2Mg_2(VO)_3(Bumal)_6(H_2O)_{15}] \cdot 2H_2O\}_n$ (**I**) with the composition and structure differed from those of the earlier described complex $\{[KMg_{0.5}(VO)(Cbdc)_2(H_2O)_{5.5}] \cdot 2.5H_2O\}_n$ with cyclobutane-1,1-dicarboxylate anions [31] and the product of the complete substitution of potassium cations by cadmium, 1D polymer $\{[Cd(VO)(Bumal)_2(H_2O)_5] \cdot H_2O\}_n$ (**II**) similar in structure to the previously described complex $\{[Mn(VO)(Bumal)_2(H_2O)_5] \cdot H_2O\}_n$ [30].

EXPERIMENTAL

New complexes were synthesized in air using distilled water, ethanol (95%), $VOSO_4 \cdot 3H_2O$ (99+%), KOH (99+%), $Mg(NO_3)_2 \cdot 6H_2O$ (98+%), $Mn(NO_3)_2 \cdot xH_2O$ (98%, Sigma Aldrich), $Cd(NO_3)_2 \cdot 4H_2O$ (99+%, Acros Organics), and H_2Bumal (99%, Sigma-Aldrich). IR spectra were recorded in a frequency range of 4000–400 cm^{-1} on a Spectrum 65 FT-IR spectrometer (PerkinElmer) equipped with a Quest ATR Accessory attachment (Specac). Elemental analysis was carried out on a EuroEA 3000 CHNS analyzer (EuroVector).

Synthesis of $\{[K_2Mg_2(VO)_3(Bumal)_6(H_2O)_{15}] \cdot 2H_2O\}_n$ (I). A solution of K_2Bumal, which was prepared by the neutralization of H_2Bumal (0.221 g, 1.38 mmol) with KOH (0.154 g, 2.76 mmol) in water (15 mL), was added to a solution of $VOSO_4 \cdot 3H_2O$ (0.15 g, 0.69 mmol) in distilled water (10 mL). The reaction mixture was stirred at 40°C for 10 min, $Mg(NO_3)_2 \cdot 6H_2O$ (0.354 g, 1.38 mmol) was added to the obtained blue solution, and the stirring was continued for 10 min. The resulting solution was kept at 22°C. Blue crystals suitable for X-ray diffraction formed in 2 months were separated from the mother liquor by filtration, washed with cold water ($T \approx 5$°C) and ethanol ($T \approx 22$°C), and dried in air. The yield of compound **I** was 0.211 g (57.9% based on $VOSO_4 \cdot 3H_2O$).

For $C_{42}H_{94}O_{44}Mg_2K_2V_3$

Anal. calcd., %	C, 31.87	H, 5.99
Found, %	C, 32.51	H, 5.75

IR (ATR; ν, cm^{-1}): 3184 vw ν(O–H), 2958 w ν(C–H), 2935 w ν(C–H), 2873 w ν(C–H), 1638 s $\nu_{as}(COO^-)$, 1583 s $\nu_{as}(COO^-)$, 1400 s $\nu_s(COO^-)$, 1348 s, 1326 s, 1304 m, 1272 m, 1245 w, 1199 m, 1116 w, 1103 s, 1006 s ν(V=O), 952 s, 892 s, 808 s δ(OCO), 774 s, 745 s, 700 vs, 613 s, 526 s, 496 s, 454 s [34, 35].

Synthesis of $\{[Cd(VO)(Bumal)_2(H_2O)_5] \cdot H_2O\}_n$ (II). A solution of K_2Bumal, which was prepared by the neutralization of H_2Bumal (0.148 g, 0.92 mmol) with KOH (0.103 g, 1.84 mmol) in water (15 mL), was added to a solution of $VOSO_4 \cdot 3H_2O$ (0.1 g, 0.46 mmol) in distilled water (10 mL). The reaction mixture was stirred at 40°C for 10 min, $Cd(NO_3)_2 \cdot 4H_2O$ (0.284 g, 0.92 mmol) was added to the obtained blue solution, and the stirring was continued for 10 min. The formed blue crystalline precipitate was filtered off, washed with water ($T \approx 22$°C), and dried in air. The crystals suitable for X-ray diffraction were obtained by the slow evaporation of the mother liquor by filtration at 22°C for 7 days. The crystals were separated from the mother liquor by filtration, washed with water ($T \approx 22$°C), and dried in air. The yield of compound **II** was 0.124 g (44.5% based on $VOSO_4 \cdot 3H_2O$).

For $C_{14}H_{32}O_{15}CdV$

Anal. calcd., %	C, 27.85	H, 5.45
Found, %	C, 27.96	H, 5.53

IR (ATR; ν, cm^{-1}): 3652 vw, 3497 w.br ν(O–H), 3371 w.br ν(O–H), 3222 w.br ν(O–H), 2960 w ν(C–H), 2930 w ν(C–H), 2870 vw ν(C–H), 1549 s $\nu_{as}(COO^-)$, 1418 s $\nu_s(COO^-)$, 1354 m, 1341 m, 1313 m, 1290 m, 1232 w, 1202 w, 1190 w, 1139 vw, 1103 w, 1071 vw, 987 s ν(V=O), 963 m, 912 w, 865 vw, 807 m δ(OCO), 772 m, 715 s, 669 m, 511 s, 486 s, 456 s, 440 s, 428 s, 420 s [34, 35].

Single crystal X-ray diffraction study of compounds **I** and **II** were carried out on a Bruker SMART APEX II diffractometer equipped with a CCD detector (MoK_α, λ = 0.71073 Å, graphite monochromator) [36]. A semiempirical absorption correction was applied [37]. The structures were solved by direct methods and refined by full-matrix least squares in the anisotropic approximation for all non-hydrogen atoms. Hydrogen atoms were generated geometrically and refined using the riding model. The calculations were performed using the SHELX-97 and SHELX-2014 program packages [38]. The crystallographic parameters and structure refinement details for compounds **I** and **II** are presented in Table 1.

The structural data for compounds **I** and **II** were deposited with the Cambridge Crystallographic Data Centre (CIF files CCDC nos. 1911220 and 1033008 for **I** and **II**, respectively); deposit@ccdc.cam.ac.uk or http://www.ccdc.cam.ac.uk/data_request/cif).

Table 1. Crystallographic data and structure refinement details for compounds **I** and **II**

Parameter	Value	
	I	**II**
FW	1582.81	602.73
T, K	153(2)	170(2)
Crystal system	Triclinic	Triclinic
Space group	$P\bar{1}$	$P\bar{1}$
a, Å	11.7871(7)	9.9366(14)
b, Å	18.3252(11)	10.6972(16)
c, Å	18.5491(11)	11.8978(17)
α, deg	65.6160(10)	83.797(2)
β, deg	74.3830(10)	65.603(2)
γ, deg	82.7430(10)	83.475(2)
V, $Å^3$	3514.0(4)	1141.7(3)
Z	2	2
ρ_{calc}, g cm^{-3}	1.496	1.753
μ, mm^{-3}	0.626	1.410
θ_{min}–θ_{max}, deg	2.19–29.47	2.62–26.05
F(000)	1658	612
T_{min}/T_{max}	0.6342/0.7459	0.5852/0.7456
Ranges of reflection indices	$-16 \le h \le 16$, $-25 \le k \le 2$, $-25 \le l \le 25$	$-12 \le h \le 12$, $-13 \le k \le 13$, $-15 \le l \le 15$
Measured reflections	39607	11117
Independent reflections	19418	5164
R_{int}	0.033	0.031
Reflections with $I > 2\sigma(I)$	15841	4189
GOOF	1.016	0.982
R factors for $F^2 > 2\sigma(F^2)$	$R_1 = 0.0908$, $wR_2 = 0.2507$	$R_1 = 0.0434$, $wR_2 = 0.1264$
R factors for all reflections	$R_1 = 0.1061$, $wR_2 = 0.2666$	$R_1 = 0.0556$, $wR_2 = 0.1377$
Residual electron density (min/max), e/$Å^3$	−3.039/3.317	−0.826/1.568

RESULTS AND DISCUSSION

The reaction of $VOSO_4 \cdot 3H_2O$, K_2Bumal, and $Mg(NO_3)_2 \cdot 6H_2O$ in a molar ratio of 1 : 2 : 2 afforded the 2D coordination polymer $\{[K_2Mg_2(VO)_3(Bumal)_6(H_2O)_{15}] \cdot 2H_2O\}_n$ (**I**). A similar reactions using $Cd(NO_3)_2 \cdot 4H_2O$ and $Mn(NO_3)_2 \cdot xH_2O$ instead of $Mg(NO_3)_2 \cdot 6H_2O$ taken in the same amounts give the 1D polymers $\{[Cd(VO)(Bumal)_2(H_2O)_5] \cdot H_2O\}_n$ (**II**) and $\{[Mn(VO)(Bumal)_2(H_2O)_5] \cdot H_2O\}_n$ (the latter was synthesized earlier using other procedure, see [30]), which have the same structures and contain no potassium cations (Scheme 1).

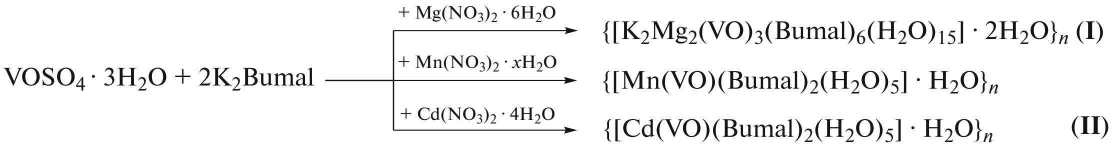

Scheme 1.

The base structural fragment of compound **I** (Fig. 1) is formed by three bis-chelate dianions $[VO(Bumal)_2(H_2O)]^{2-}$ containing crystallographically nonequivalent vanadium atoms (V(1), V(2), and V(3)), two magnesium atoms (Mg(1) and Mg(2)), two potassium atoms (K(1) and K(2)), and fifteen water molecules coordinated to the metal atoms. A similar structure of the elementary unit (three bis-chelate dianions with nonequivalent vanadium atoms) was observed earlier in the structures of the Ba–V [30], Sr–V [39], and Na–V [40] compounds with $Bumal^{2-}$ anions. The vanadium atom of each $[VO(Bumal)_2(H_2O)]^{2-}$ dianion is in the distorted octahedral coordination environment of six O atoms. The equatorial plane of the polyhedron is occupied by the O atoms of the carboxyl groups of two butylmalonate anions coordinated via the chelate mode, and the O atom of the vanadyl group and the O atom of the water molecule are located in the axial positions. The bond lengths and bond angles characterizing the coordination polyhedra of vanadium lie in the ranges observed for other known substituted oxovanadium(IV) malonates (Table 2) [30, 31, 39–45]. Within one elementary unit, the metal fragments $[V(3)O(Bumal)_2(H_2O)]^{2-}$ and $[V(2)O(Bumal)_2(H_2O)]^{2-}$ bind the Mg(1) and Mg(2) magnesium atoms due to the coordination of the carboxyl groups of the butylmalonate anions, whereas the K(1) atom links the Mg(1) atom with the bis-chelate dianions $[V(1)O(Bumal)_2(H_2O)]^{2-}$ and $[V(2)O(Bumal)_2(H_2O)]^{2-}$ due to the coordination of two bridging water molecules and four O atoms of the carboxyl groups of the vanadium-containing fragments. Each of the Mg(2), K(1), and K(2) atoms also coordinates one carboxylate O atom of the metal fragments $[V(1)O(Bumal)_2(H_2O)]^{2-}$, $[V(2)O(Bumal)_2\text{-}(H_2O)]^{2-}$, and $[V(3)O(Bumal)_2(H_2O)]^{2-}$, respectively, belonging to the adjacent units and thus links the elementary structural fragments into the layered polymeic structure (Fig. 2), which is additionally stabilized due to hydrogen bonds (Table 3). The distances between the vanadium atoms V(1)···V(2), V(2)···V(3), and V(3)···V(1) in the elementary structural fragment are 7.882, 7.652, and 11.583 Å, respectively. The Mg(1) atom is in the octahedral coordination environment: it coordinates five water molecules along with one carboxylate O atom of the $[V(3)O(Bumal)_2(H_2O)]^{2-}$ dianion. Two water molecules (O(9*w*) and O(10*w*)) are bridging and bind the Mg(1) atom to the K(1) atom, whereas three water molecules (O(1*w*), O(3*w*), and O(11*w*)) are coordinated in the monodentate mode. The octahedral environment of the Mg(2) atom is formed by two carboxylate O atoms of the metal fragments $[V(1)O(Bumal)_2(H_2O)]^{2-}$ and $[V(2)O(Bumal)_2(H_2O)]^{2-}$ belonging to the adjacent structural units and by four water molecules, one of which is bridging (O(15*w*)) and binds the Mg(2) atom to the K(2) atom, whereas three water molecules (O(13*w*), O(14*w*), and O(16*w*)) are coordinated in the monodentate mode. The values of the main angles in the Mg polyhedra are presented in Table 2. The K(2) atom additionally coordinates three water molecules (O(4*w*), O(6*w*), and O(7*w*)) in the monodentate mode.

In spite of similar procedures for the synthesis of the earlier obtained 1D polymer $\{[KMg_{0.5}(VO)(Cbdc)_2(H_2O)_{5.5}] \cdot 2.5H_2O\}_n$ and new 2D polymer $\{[K_2Mg_2(VO)_3(Bumal)_6(H_2O)_{15}] \cdot 2H_2O\}_n$ (**I**), their compositions and structures are absolutely different, which can be due to both the nature of the carboxylate anion (steric effect of the substituent in the malonate ligand) and the ratio of metals in the structure. The K : Mg : V ratio in the elementary fragment of the compound with the $Cbdc^{2-}$ anions is 1 : 0.5 : 1, and that in compound **I** is 2 : 2 : 3. Thus, the content of Mg in the elementary unit of compound **I** is by four times higher than that in cyclobutane-1,1-dicarboxylate, whereas the vanadium content is by three times higher than that in cyclobutane-1,1-dicarboxylate, which favored, most likely, the formation of the structure of a higher dimensionality in spite of the presence of the bulky butyl substituent in the malonate anion.

The polymeric chains of compound **II** are formed by the $\{VO(Bumal)_2(H_2O)\}$ fragments similar in structure to the bis-chelate blocks of compound **I** (Fig. 3, Table 2), and all vanadium atoms in the structure are crystallographically equivalent. The metal fragments $\{VO(Bumal)_2(H_2O)\}$ are bound into polymeric chains by the cadmium atoms, each of which coordinates two carboxylate O atoms of the ligand of the adjacent bis-chelate vanadium-containing fragments. Unlike the previously obtained compound $\{[Cd(VO)(Cbdc)_2(H_2O)_5] \cdot H_2O\}_n$ [44] in which the dicarboxylic acid anions of the $\{VO(Cbdc)_2(H_2O)\}$ fragment manifest different coordination modes (μ_3,κ^2-chelate bridging, and κ^2-chelate), both acid anions of the $\{VO(Bumal)_2(H_2O)\}$ fragment in compound **II** demonstrate the μ,κ^2 coordination mode. The interatomic distances V(1)···Cd(1) and V(1)···Cd(2) in the polymeric chain are not equal being 5.155 and 5.089 Å, respectively, whereas the distances between the adjacent cadmium atoms are the same and equal to 9.235 Å, which is by ~1.34 Å longer than that in $\{[Cd(VO)(Cbdc)_2(H_2O)_5] \cdot H_2O\}_n$. In addition, unlike V–Cd cyclobutane-1,1-dicarboxylate, the V···V distances in compound **II** are different and elongated by ~2.4 Å (10.178 and 10.311 Å). The crystal structure of compound **II** is additionally stabilized due to hydrogen bonds, whose formation involves the solvate and coordinated water molecules and the O atoms of the carboxyl groups (Table 4). The structure of compound **II** contains crystallographically nonequivalent cadmium atoms of two types, Cd(1) and Cd(2), with different characteristics of the octahedral coordination

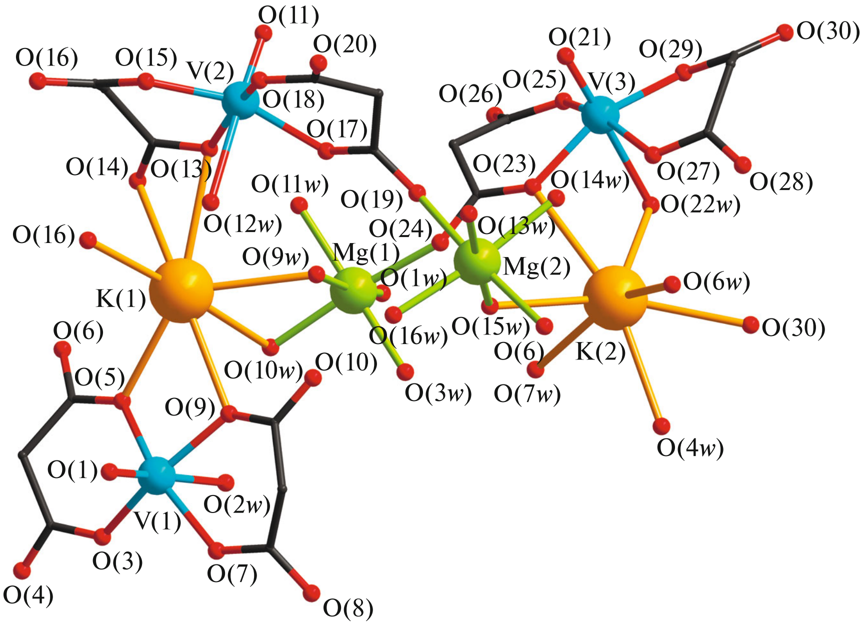

Fig. 1. Base fragment of the 2D polymeric structure of compound **I**. Butyl substituents of the acid anions and hydrogen atoms are omitted.

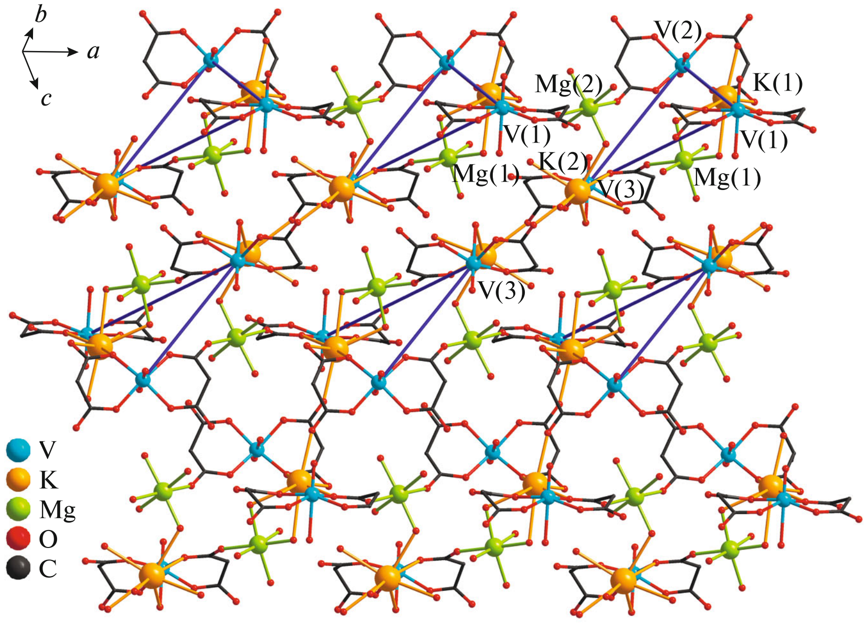

Fig. 2. Structure of the polymeric layer in compound **I**. Blue lines connect the V(1), V(2), and V(3) atoms of the elementary units. Butyl substituents and hydrogen atoms are omitted.

polyhedra. The equatorial plane of the Cd(1) polyhedron is formed by four O atoms of the water molecules coordinated in the monodentate mode (two O(3*w*) and two O(4*w*)), and the axial positions are occupied by the O(7) atoms of the carboxyl groups of the butylmalonate anions of the $\{VO(Bumal)_2(H_2O)\}$ bis-chelate fragments. In the Cd(2) polyhedron, the carboxylate O(5) atoms of the bis-chelate fragments $\{VO(Bumal)_2(H_2O)\}$ lie in the equatorial plane together with two O atoms of the water molecules coordinated in the monodentate mode (two O(2*w*)), and two other O atoms of the water molecules

Table 2. Selected bond lengths (d, Å) and bond angles (ω, deg) characterizing the coordination polyhedra of vanadium (CP_V), magnesium and cadmium ($CP_{Mg, Cd}$) in compounds **I** and **II**

Bond	d, Å	
	I (M = Mg)	**II** (M = Cd)
V=O	1.586(3), 1.593(3), 1.595(3)	1.580(3)
V–O (Bumal)	1.987(3)–2.023(3)	1.986(2)–2.003(3)
V–O (H_2O)	2.321(3), 2.326(3), 2.363(3)	2.316(3)
M–O (Bumal)	2.060(3), 2.079(3), 2.085(3)	2.323(2), 2.327(3)
M–O (H_2O)	2.034(3)–2.095(3)	2.238(3)–2.303(3)
K–O (Bumal)	2.698(3)–3.024(3)	
K–O (H_2O)	2.761(3)–3.100(3)	

CP_V

Angle	ω, deg	
	I (M = V)	**II** (M = V)
$O_{oxo}VO_{eq}$	98.42(15)–102.14(16)	99.20(13)–102.47(13)
$O_{oxo}VO_{ax}$	176.48(15), 177.89(15), 179.17(15)	175.68(14)
$O_{eq}VO_{eq}$ (adjacent)	86.64(12)–91.24(12)	84.74(10)–89.32(10)
$O_{eq}VO_{ax}$	77.51(11)–81.86(12)	75.87(11)–82.19(11)

$CP_{Mg, Cd}$

Angle	ω, deg	
	I (M = Mg)	**II** (M = Cd)
$O_{ax}MO_{eq}$	83.69(12), 86.79(13)–96.12(14)	80.64(10), 85.68(11)–94.32(11), 99.36(10)
$O_{eq}MO_{eq}$ (adjacent)	82.32(12), 86.88(15)–96.96(13)	80.49(10), 87.18(12), 92.82(12), 99.51(10)
$O_{ax}MO_{ax}$	170.48(14), 177.27(15)	180

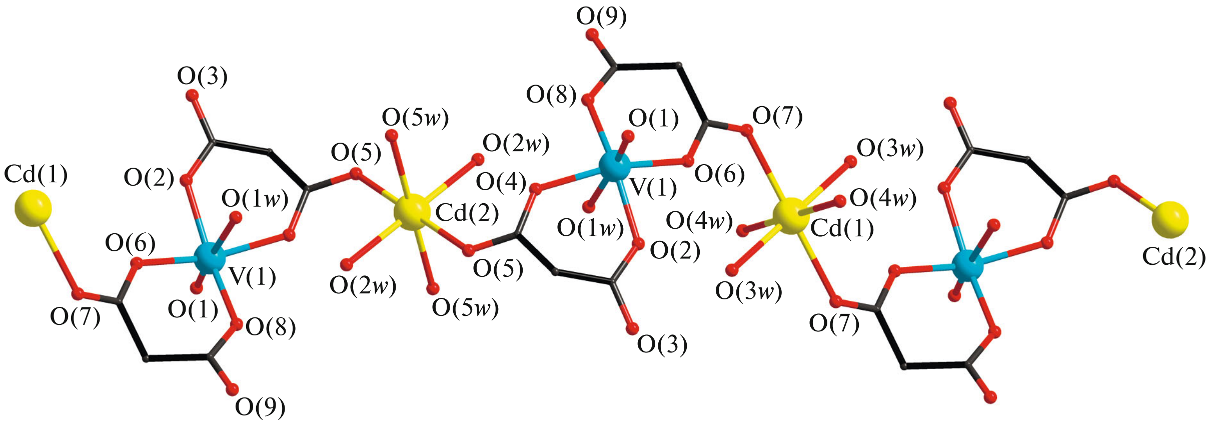

Fig. 3. Structure of the polymeric chain in complex **II**. Butyl substituents of the acid anions and hydrogen atoms are omitted.

Table 3. Geometric parameters of hydrogen bonds in the structure of compound **I***

D–H···A	Distance, Å			Angle D–H···A, deg
	D–H	H···A	D···A	
O(3*w*)–H(3*w*a)···O(8)$^{(i)}$	0.83	1.88	2.706	176
O(5*w*)–H(5*w*b)···(O1)$^{(ii)}$	0.83	2.26	3.069	168
O(5*w*)–H(5*w*a)···O(4*w*)$^{(iii)}$	0.83	2.05	2.815	153
O(16*w*)–H(16c)···O(10)$^{(iv)}$	0.83	1.94	2.749	164
O(11*w*)–H(11c)···O(28)$^{(iv)}$	0.83	2.01	2.826	171
O(2*w*)–H(2*w*a)···O(8)$^{(v)}$	0.83	1.94	2.702	152
O(1*w*)–H(1*w*a)···O(29)$^{(vi)}$	0.83	2.18	2.859	140
O(12*w*)–H(12c)···O(20)$^{(ii)}$	0.83	1.98	2.771	159
O(11*w*)–H(11d)···O(13)	0.83	2.06	2.886	179
O(16*w*)–H(16d)···O(20)$^{(ii)}$	0.83	1.96	2.782	176
O(2*w*)–H(2*w*b)···O(4)$^{(i)}$	0.83	1.98	2.795	168
O(4*w*)–H(4*w*a)···O(4)$^{(i)}$	0.83	1.99	2.820	174
O(3*w*)–H(5*w*b)···O(7*w*)	0.83	1.89	2.712	169
O(22*w*)–H(22d)···O(28)$^{(vii)}$	0.83	2.29	3.093	163
O(15*w*)–H(15d)···O(8*w*)	0.83	1.82	2.639	169
O(1*w*)–H(1*w*b)···O(25)$^{(vi)}$	0.83	1.94	2.730	158
O(10*w*)–H(10d)···O(2*w*)$^{(iv)}$	0.83	2.10	2.902	162
O(9*w*)–H(9*w*b)···O(17)	0.83	1.93	2.760	177
O(8*w*)–H(8*w*a)···O(7)$^{(i)}$	0.83	2.06	2.819	152
O(8*w*)–H(8*w*b)···O(3)$^{(i)}$	0.83	2.19	2.853	137
O(14*w*)–H(14e)···O(14)$^{(viii)}$	0.83	1.84	2.654	167
O(13*w*)–H(13c)···O(15)$^{(ii)}$	0.83	2.40	2.850	115
O(13*w*)–H(13d)···O(18)$^{(ii)}$	0.83	1.97	2.778	164
O(14*w*)–H(14d)···O(27)	0.83	2.39	3.059	138

* Symmetry codes: ^{i} $-x + 2, -y + 2, -z$; ^{ii} $-x + 1, -y + 2, -z + 1$; ^{iii} $x - 1, y, z + 1$; ^{iv} $x - 1, y, z$; ^{v} $-x + 3, -y + 2, -z$; ^{vi} $-x + 1, -y + 3, -z$; ^{vii} $-x + 2, -y + 3, -z$; ^{viii} $x + 1, y, z$.

(O(5*w*)) are located in the axial positions. The values of the main angles in the Cd polyhedra are presented in Table 2.

The consideration of the crystal packing of the polymeric chains shows that the distances between the Cd atoms of the adjacent chains are shorter than the Cd···Cd distances within one chain by 3.29 Å (5.949 Å), whereas the corresponding interatomic V···V distances are shorter by 2.9 Å (7.403 and 7.436 Å).

The structure and packing of the polymeric chains in the crystal of compound **II** are similar to the structure and packing of the chains in the crystal of its manganese-containing analog $\{[Mn(VO)(Bumal)_2(H_2O)_5] \cdot H_2O\}_n$ synthesized by the substitution of the barium(II) cations (see [30]) (Fig. 4). This indicates that the radius of the *d*-metal cation exerts no effect on the structure of the heterometallic compound formed by the bis-chelate vanadyl fragments as it was observed for the compounds with cyclobutane-1,1-dicarboxylate anions (see [44]).

Thus, like for copper(II) malonates, for the systems with oxidovanadium(IV), only the partial substitution of potassium cations by magnesium is shown to occur, regardless of the nature of the substituent in the malonate anion [28]. The $\{[K_2Mg_2(VO)_3(Bumal)_6(H_2O)_{15}] \cdot 2H_2O\}_n$ complex (**I**) with butylmalonate anions containing the bulky substituent has a higher dimensionality (2D) than the corresponding compound with cyclobutane-1,1-dicarboxylate anions $\{[KMg_{0.5}(VO)(Cbdc)_2(H_2O)_{5.5}] \cdot 2.5H_2O\}_n$ having the 1D structure. This effect is most likely can be explained by the fact that the elementary fragment of compound **I** contains more metall centers capable of

Table 4. Parameters of hydrogen bonds in the structure of compound **II***

D–H···A	Distance, Å			Angle D–H···A, deg
	D–H	H···A	D···A	
O(1*w*)–H(1*w*1)···O(3)$^{\rm i}$	0.83	1.84	2.659	169
O(1*w*)–H(2*w*1)···O(9)$^{\rm ii}$	0.83	1.92	2.688	155
O(2*w*)–H(1*w*2)···O(1*w*)	0.83	2.10	2.893	160
O(2*w*)–H(2*w*2)···O(7)$^{\rm iii}$	0.83	2.05	2.838	159
O(3*w*)–H(1*w*3)···O(2)$^{\rm iv}$	0.83	2.16	2.975	164
O(3*w*)–H(2*w*3)···O(5)$^{\rm v}$	0.83	2.02	2.835	165
O(4*w*)–H(1*w*4)···O(9)$^{\rm ii}$	0.83	1.87	2.701	176
O(4*w*)–H(2*w*4)···O(6*w*)	0.83	2.19	2.836	134
O(5*w*)–H(1*w*5)···O(6*w*)$^{\rm ii}$	0.83	1.98	2.768	160
O(5*w*)–H(2*w*5)···O(3)$^{\rm vi}$	0.83	1.89	2.711	170
O(6*w*)–H(1*w*6)···O(8)$^{\rm ii}$	0.83	2.22	2.924	142
O(6*w*)–H(1*w*6)···O(2*w*)$^{\rm ii}$	0.83	2.63	3.138	121

* Symmetry codes: $^{\rm i}$ $-x + 1, -y, -z + 1$; $^{\rm ii}$ $-x + 1, -y, -z$; $^{\rm iii}$ $-x + 2, -y, -z$; $^{\rm iv}$ $x + 1, y, z - 1$; $^{\rm v}$ $x - 1, y, z$.

binding the bis-chelate vanadium-containing fragments between each other. At the same time, the potassium cations are completely substituted upon the interaction with magnesium and cadmium in spite of a substantial difference in their ion radii. The formed 1D polymeric complexes of the formula $\{[M(VO)(Bumal)_2(H_2O)_5] \cdot H_2O\}_n$ (M = Mn, Cd) have the same structures.

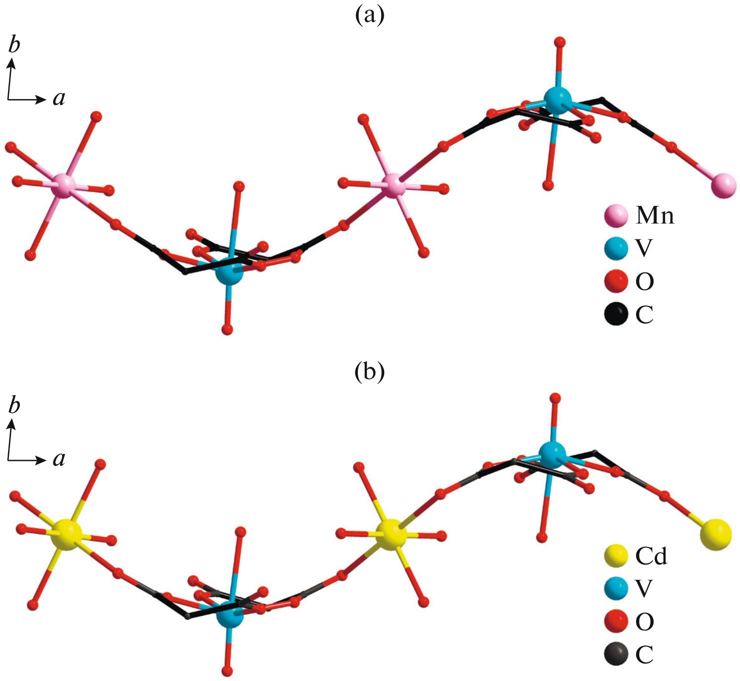

Fig. 4. Comparison of the structures of the polymeric chains in compounds (a) $\{[Mn(VO)(Bumal)_2(H_2O)_5] \cdot H_2O\}_n$ and (b) **II**. Butyl substituents of the acid anions and hydrogen atoms are omitted.

ACKNOWLEDGMENTS

Elemental CHNS analyses, IR spectroscopy, and X-ray structure analysis were carried out using Shared Experimental Facilities of the Kurnakov Institute of General and Inorganic Chemistry (Russian Academy of Sciences) supported by IGIC RAS State Assignment.

FUNDING

This work was supported by the Russian Science Foundation, project no. 19-73-10181.

CONFLICT OF INTEREST

The authors declare that they have no conflicts of interest.

REFERENCES

1. Papatriantafyllopoulou, C., Wernsdorfer, W., Abboud, K.A., and Christou, G., *Inorg. Chem.*, 2011, vol. 50, p. 421.
2. Langley, S.K., Wielechowski, D.P., Vieru, V., et al., *Angew. Chem., Int. Ed. Engl.*, 2013, vol. 52, p. 12014.
3. Zhao, F.-H., Li, H., Che, Y.-X., et al., *Inorg. Chem.*, 2014, vol. 53, p. 9785.
4. Pineda, E.M., Chilton, N.F., Tuna, F., et al., *Inorg. Chem.*, 2015, vol. 54, p. 5930.
5. Kiskin, M., Zorina-Tikhonova, E., Kolotilov, S., et al., *Eur. J. Inorg. Chem.*, 2018, p. 1356.
6. Fan, S., Xu, S., Zheng, X., et al., *CrystEngComm*, 2018, vol. 20, p. 2120.
7. Botezat, O., van Leusen, J., Kogerler, P., and Baca, S.G., *Eur. J. Inorg. Chem.*, 2019, p. 2236.
8. Yin, M., Lei, X., Li, M., et al., *J. Phys. Chem. Solids*, 2006, vol. 67, p. 1372.
9. Bo, Q.-B., Wang, H.-Y., Wang, D.-Q., et al., *Inorg. Chem.*, 2011, vol. 50, p. 10163.
10. Goldberg, A., Kiskin, M., Shalygina, O., et al., *Chem. Asian J.*, 2016, vol. 11, p. 604.
11. Kiskin, M.A., Dobrokhotova, Zh.V., Bogomyakov, A.S., et al., *Russ. Chem. Bull., Int. Ed.*, 2016, vol. 65, no. 6, p. 1488.
12. Zheng, S.-R., Tan, J.-B., Cai, S.-L., et al., *CrystEngComm*, 2016, vol. 18, p. 8672.
13. Kiraev, S.R., Nikolaevskii, S.A., Kiskin, M.A., et al., *Inorg. Chim. Acta*, 2018, vol. 477, p. 15.
14. Hou, S., Tang, X.-Y., Li, Y., et al., *J. Mol. Struct.*, 2018, vol. 1167, p. 239.
15. Nesterov, D.S., Nesterova, O.V., and Pombeiro, A.J.L., *Coord. Chem. Rev.*, 2018, vol. 355, p. 199.
16. Wei, L.-Q. and Ye, B.-H., *Inorg. Chem.*, 2019, vol. 58, p. 4385.
17. Kuhn, P.-S., Cremer, L., Gavriluta, A., et al., *Chem.-Eur. J.*, 2015, vol. 21, p. 13703.
18. Shi, F.-N., Pinto, M.L., Ananias, D., and Rocha, J., *Micropor. Mesopor. Mat.*, 2014, vol. 188, p. 172.
19. Ding, Y.-J., Li, T., Hong, X.-J., et al., *CrystEngComm*, 2015, vol. 17, p. 3945.
20. Sapianik, A.A., Zorina-Tikhonova, E.N., Kiskin, M.A., et al., *Inorg. Chem.*, 2017, vol. 56, p. 1599.
21. Zou, J., Li, L., You, S., et al., *Dalton Trans.*, 2017, vol. 46, p. 16432.
22. Feng, X., Feng, Y., Guo, N., et al., *Inorg. Chem.*, 2017, vol. 56, p. 1713.
23. Sapchenko, S.A., Demakov, P.A., Samsonenko, D.G., et al., *Chem.-Eur. J.*, 2017, vol. 23, p. 2286.
24. Zhao, S., Hao, X.-M., Liu, J.-L., et al., *J. Solid State Chem.*, 2017, vol. 255, p. 76.
25. Litvinova, Yu.M., Gayfulin, Y.M., Kovalenko, K.A., et al., *Inorg. Chem.*, 2018, vol. 57, p. 2072.
26. Bolotov, V.A., Kovalenko, K.A., Samsonenko, D.G., et al., *Inorg. Chem.*, 2018, vol. 57, p. 5074.
27. Dobrokhotova, Zh.V., Gogoleva, N.V., Zorina-Tikhonova, E.N., et al., *Eur. J. Inorg. Chem.*, 2015, p. 3116.
28. Gogoleva, N.V., Zorina-Tikhonova, E.N., Bogomyakov, A.S., et al., *Eur. J. Inorg. Chem.*, 2017, p. 547.
29. Bazhina, E.S., Gogoleva, N.V., Zorina-Tikhonova, E.N., et al., *J. Struct. Chem.*, 2019. vol. 6, no. 6, p. 855.
30. Bazhina, E.S., Aleksandrov, G.G., Bogomyakov, A.S., et al., *Polyhedron*, 2014, vol. 77, p. 47.
31. Bazhina E.S., Aleksandrov, G.G., Kiskin, M.A., et al., *Russ. J. Coord. Chem.*, 2017, vol. 43, no. 11, p. 709. https://doi.org/10.7868/S0132344X17110019
32. Gogoleva, N.V., Zorina-Tikhonova, E.N., Bogomyakov, A.S., et al., *Eur. J. Inorg. Chem.*, 2017, p. 547.
33. Zauzolkova, N.V., Zorina, E.N., Sidorov, A.A., et al., *Russ. Chem. Bull., Int. Ed.*, 2012, vol. 61, no. 7, p. 1419.
34. Nakamoto, K., *Infrared Spectra of Inorganic and Coordination Compounds*, New York: Wiley, 1963.
35. Bellamy, L.J., *The Infrared Spectra of Complex Molecules*, New York: Wiley, 1958.
36. *SMART (control) and SAINT (integration) Software. Version 5.0.* Madison (WI, USA): Bruker AXS, Inc., 1997.
37. Sheldrik, G.M., *SADABS. Program for Scanning and Correction of Area Detector Data*, Göttingen: Univ. of Göttingen, 2004.
38. Sheldrick, G.M., *Acta Crystallogr., Sect. A: Found. Crystallogr.*, 2008, vol. 64, p. 112.
39. Bazhina, E.S., Aleksandrov, G.G., Sidorov, A.A., and Eremenko, I.L., *Russ. J. Coord. Chem.*, 2015, vol. 41, no. 11, p. 730. https://doi.org/10.7868/S0132344X15110018
40. Bazhina, E.S., Aleksandrov, G.G., Kiskin, M.A., et al., *Russ. Chem. Bull., Int. Ed.*, 2014, vol. 63, no. 7, p. 1475.
41. Bazhina, E.S., Nikiforova, M.E., Aleksandrov, G.G., et al., *Russ. Chem. Bull., Int. Ed.,* 2011, vol. 60, no. 5, p. 797.
42. Bazhina, E.S., Aleksandrov, G.G., Efimov, N.N., et al., *Russ. Chem. Bull., Int. Ed.*, 2013, vol. 62, no. 4, p. 962.
43. Bazhina, E.S., Aleksandrov, G.G., Kiskin, M.A., et al., *Russ. Chem. Bull., Int. Ed.,* 2016, vol. 65, no. 1, p. 249.
44. Bazhina, E.S., Gogoleva, N.V., Aleksandrov, G.G., et al., *Chem. Select.*, 2018, p. 13765.
45. Bazhina, E.S., Aleksandrov, G.G., Kiskin, M.A., et al., *Eur. J. Inorg. Chem.*, 2018, p. 5075.

Translated by E. Yablonskaya